STUDY OF THE NONSTEADY PROPAGATION OF AN IONIZING SHOCK WAVE IN A MAGNETIC FIELD

A. A. Barmin and V. S. Uspenskii

UDC 533.6.011:537.84+537.56

The study of ionizing shock waves (SW) in a magnetic field [1] has shown that an electromagnetic wave is generated in front of the discontinuity. This wave creates a nontrivial intrinsic electric field in particles ahead of it. The theory which was developed – according to which ionization occurs as a result of heating in the gas dynamic discontinuity – has reliably described the behavior of ionizing waves of moderate intensity seen in experiments [2, 3]. One feature of strong SWs in a magnetic field (at velocities D > 3 km/sec) observed in experiments is the formation ahead of the shock wave of a region in which the magnetic field undergoes a change. The existence of this region is evidence of the presence of an electrically conducting medium ahead of the shock [4, 5]. The observed effects of the change in the magnetic field cannot be explained by considering only advance photoionizating radiation in the continuous spectrum as the source of ionization in the cold gas (as in normal gas dynamics) [6]. In contrast to gas dynamics, the presence of an electric field in front of the shock leads to heating of free electrons. Thus, not only does ionization occur as a result of electron collision [7], but also the high electron temperature prevents the free electrons formed as a result of photoionization from recombining – despite the low temperature of the heavy particles. The formation of a conducting zone ahead of the shock wave in turn leads to screening of the electric field generated by the discontinuity. This fact was not considered in [7]. Here, we perform a numerical calculation of the problem on the basis of a model of the phenomenon adapted to the conditions of the experiment in [4]. Our goal is to qualitatively substantiate the model.

1. Formulation of the Problem. We will examine a region occupied by nonelectrically conducting hydrogen in a magnetic field and bounded by a plane (or cylindrical) nonradiating wall and a piston. The wall is assumed to be nonelectrically conducting, and a constant initial value of the magnetic field H_0 is maintained on it; the piston is ideally conducting, and the value of the electric field on it is $E = 0$. The vector of the magnetic field is assumed to be parallel to the plane of the piston. At the moment of time, $t = 0$, the piston acquires a constant velocity $u_p > 0$. We need to find the distribution of the physical parameters in the flow up to the moment the SW that is created is reflected from the walls.

The system of equations and the initial and boundary conditions describing the unidimensional flow of an ideal gas in plane waves has the same form as in [6, 8] in Lagrangian variables. Below we use the system of equations of unidimensional magnetohydrodynamics, ionization kinetics, and radiative transfer to study the nonsteady propagation of strong ionizing SWs in a magnetic field in the case when the processes discussed above are significant ahead of the shock. One feature of the calculations is the presence of two regions – a high-temperature region behind the shock wave and a low-temperature region ahead of it, where ionization and radiative transfer become particularly important:

$$\partial r/\partial t = u; \tag{1.1}$$

$$\frac{\partial}{\partial t}\left(\frac{1}{\rho}\right) = \frac{\partial}{\partial s}\left(r^{\nu-1}u\right); \tag{1.2}$$

$$\frac{\partial u}{\partial t} = -r^{\nu-1}\frac{\partial}{\partial s}\left(p + \frac{H^2}{8\pi}\right); \tag{1.3}$$

$$\frac{\partial \varepsilon}{\partial t} = -p\frac{\partial\left(r^{\nu-1}u\right)}{\partial s} + \frac{\sigma E^2}{\rho} - \frac{S}{\rho}; \tag{1.4}$$

$$\frac{\partial H}{\partial s} = -\frac{4\pi\sigma}{c\rho r^{\nu-1}}E; \tag{1.5}$$

Moscow. Translated from Zhurnal Prikladnoi Mekhaniki i Tekhnicheskoi Fiziki, No. 3, pp. 20-26, May-June, 1989. Original article submitted August 19, 1987; revision submitted January 11, 1988.

0021-8944/89/3003-0356$12.50

$$\frac{\partial}{\partial t}\left(\frac{H}{\rho}\right) = -\frac{\partial}{\partial s}(cr^{\nu-1}E); \tag{1.6}$$

$$\frac{\partial \alpha}{\partial t} = \dot{\alpha}_{co} + \dot{\alpha}_{pht}; \tag{1.7}$$

$$\frac{1}{r^{\nu-1}}\frac{\partial}{\partial \tau^2}(r^{\nu-1}q) - 4q = 4\pi\frac{\partial r^{\nu-1}S_{pht}}{r^{\nu-1}\partial\tau}; \tag{1.8}$$

$$\sigma E^2 = NkJ\dot{\alpha}_{co} + Q_\Delta k(T_e - T)\alpha. \tag{1.9}$$

Here, r and s are Eulerian and Lagrangian space coordinates; $\nu = 1$ corresponds to plane geometry, while $\nu = 2$ corresponds to cylindrical geometry; ρ, p, and ε are the density, pressure, and internal energy of a unit mass of gas; u is velocity; σ is electrical conductivity; H and E are the strengths of the magnetic and electric fields; α is the degree of ionization of the gas; $\dot{\alpha}_{co}$ and $\dot{\alpha}_{pht}$ are the source terms in the ionization kinetics equation accounting for the formation and loss of free electrons in collision and radiation processes; q is the continuous-spectrum radiant flux; τ is the optical thickness of the radiating gas; S_{pht} is the modified Planck radiation function; N is the number of heavy particles per unit volume; k is the Boltzmann constant; c is the speed of light; T and T_e are the temperatures of the heavy particles and electrons; J is the ionization potential of the atoms in the gas; S is the unit radiative heat supply. The equations of state of the medium for the gas will be written in the form

$$\varepsilon = \frac{1}{\gamma - 1}\frac{k}{m_a}T + \frac{3}{2}\alpha\frac{k}{m_a}T_e + \alpha\frac{k}{m_a}J + \beta\frac{k}{m_a}E_{dis}; \tag{1.10}$$

$$p = \rho\frac{k}{m_a}(T + \alpha T_e), \tag{1.11}$$

where γ is the ratio of the heat capacities, equal to 5/3 for a monatomic gas and 1.4 for a diatomic gas; β and E_{dis} are the degree and energy of dissociation of hydrogen. The optical density is determined by the relation

$$\tau = rk_\nu, \quad k_\nu = 0.96\cdot 10^{-7}\frac{2NkJ}{(\hbar\nu/kJ)^3}\ (\text{cm}^{-1}) \tag{1.12}$$

(k_ν is the coefficient of absorption of radiation with the frequency ν for quanta with the energy $\hbar\nu \geq kJ$ (Unsold–Kramers formula [9])).

We will use the following relations and values [6, 10-12] for the transport coefficients and constants in Eqs. (1.1)-(1.10):

$$\sigma = \frac{e^2\alpha}{m_e\nu_{eff}/N}, \quad \nu_{eff} = \left(\frac{8kT_e}{\pi m_e}\right)^{1/2} N[(1-\alpha)\sigma_{ea} + \alpha\sigma_{ei}], \tag{1.13}$$

$$Q_\Delta = \frac{3m_e}{m_a}\nu_{eff}, \quad \dot{\alpha}_{pht} = -\frac{1}{NkJr^{\nu-1}}\frac{\partial r^{\nu-1}q}{\partial r},$$

$$\dot{\alpha}_{co} = (\alpha k_{fe} + (1-\alpha)k_{fa})(1 - \alpha - \alpha^2 N/k_{eq}),$$

$$S_{pht} = \frac{\alpha^2(1-\alpha_{eq})}{\alpha_{eq}^2(1-\alpha)}\int_{kJ/\hbar}^{\infty}\frac{2\nu^3}{c^2}\exp\left(-\frac{\hbar\nu}{kT_e}\right)d\nu,$$

$$k_{fe}^{-1} = k_{fe2}^{-1} + k_{fe1}^{-1}\chi(E_2/T_e), \quad 5\cdot 10^3 < T_e < 2\cdot 10^4\ \text{K},$$

$$\chi(x) = \frac{4}{3\sqrt{x}}\int_0^x \exp(-t)\,t^{3/2}dt,$$

$$k_{eq} = 2.4\cdot 10^{15}T_e^{3/2}\exp(-J/T_e)\ \ (\text{cm}^{-3}),$$

$$k_{fe1} = 1.3\cdot 10^{-5}T_e^{-3}\exp(-J/T_e)N\ \ (\text{cm}^3/\text{sec}),$$

$$T_e < 5\cdot 10^3\ \text{K},\ k_{fe2} = 2.55\cdot 10^{-13}(2 + E_2/T_e)\exp(-E_2/T_e)N\ \ (\text{cm}^3/\text{sec}),$$

$$2\cdot 10^4 < T_e < 6\cdot 10^4\ \text{K},$$

$$k_{fa} = 2.9\cdot 10^{10}T^{-1}\exp(-J/T)\sigma_{ea}N\ \ (\text{cm}^3/\text{sec}).$$

$$\sigma_{ea} = \begin{cases}(12.49 + 21.42\lg T_e - 5.01\lg^2 T_e)\cdot 10^{-16}\ \ (\text{cm}^2),\ T_e < 2\cdot 10^4\ \text{K},\\ (1.38\cdot 10^5 T_e^{-1} + 714.2T_e^{-1/2})\cdot 10^{-16}\ \ (\text{cm}^2),\ T_e \geqslant 2\cdot 10^4\ \text{K}.\end{cases}$$

Here, ν_{eff} is the effective frequency of collision of an electron with heavy particles; α_{eq} is the equilibrium degree of ionization corresponding to the current values of ρ and T_e; k_{eq} is the constant for the ionization process; k_{fe1}, k_{fe2}, and k_{fe} are the rates of ionization by electron collision; k_{fa} is the rate of ionization in interatomic collisions; the ionization potential of a hydrogen atom $J = 1.556 \cdot 10^5$ K; the energy of the first excited state $E_2 = 1.18 \cdot 10^5$ K; $E_{dis} = 5.197 \cdot 10^4$ K. The hydrogen plasma is transparent in the lines [13]. For $N \sim 10^{16}$ cm^{-3}, $k_\nu \lesssim 10$ cm^{-1}. In the heat flux equation (1.4), only radiative transfer of the continuous spectrum is considered because $S = -(1/r^{\nu-1})(\partial r^{\nu-1} q/\partial r)$. The absorption coefficient for the radiation of the continuous spectrum is assumed to be independent of the spectral frequency and is calculated from (1.12) with $\hbar\nu = kJ$.

We will use the semiempirical Townsend theory [12] to describe ionization by electron collision ahead of the shock wave. We do this because the electron energy distribution during the initial stage of ionization differs from the Maxwell distribution, making it impossible to use established dependences of ionization rate on electron temperature [10]. In this case,

$$k_{fe} = T_a V_d, \tag{1.14}$$

where T_a is the first Townsend ionization coefficient; V_d is the rate of drift of free electrons in the external electric field. For example, for hydrogen in an external electric field under the conditions $E/p \in (1.2; 4)$ W·cm^{-1}·Pa^{-1}, we obtain [14] $T_a = pA\exp(-Bp/E)$, $A = 0.04$ cm^{-1}·Pa^{-1}, $B = 1$ V·cm^{-1}·Pa^{-1}. For V_d, we took values tabulated in [15] as a function of E/p. The criterion of the existence of a Maxwell distribution is $c_M \ll 1$ [10]: $c_M = 0.5 \cdot 10^{-3}\alpha^{-1} \cdot T_e(1 + T_e/(J - E_2))/(J - E_2)$.

We used (1.14) at $c_M > 1$ and (1.13) at $c_M < 1$ in the calculations. The boundary and initial conditions:

$$s = 0,\ u = u_p,\ E = 0,\ \frac{1}{r^{\nu-1}}\frac{\partial r^{\nu-1} q}{\partial \tau} - 2q = 4\pi S_{pht}; \tag{1.15}$$

$$s = s_0 \equiv (L^\nu - r_0^\nu)\pi^{\nu-1}\rho_0,\ u = 0,\ H = H_0, \quad \frac{1}{r^{\nu-1}}\frac{\partial r^{\nu-1} q}{\partial \tau} + 2q = 4\pi S_{pht}, \tag{1.16}$$

$t = 0$, $0 \le s \le s_0$, $T = T_e = T_0$, $\rho = \rho_0$, $u = 0$, $E = 0$, $H = H_0$ (u_p is the velocity of the piston and L is the size of the unit). Conditions (1.15) and (1.16) correspond to the assumption that the piston and the wall do not radiate [16].

2. Features of the Calculations. An experiment set up to create powerful ionizing shock waves in a magnetic field was described in [4]. An electric discharge was initiated in a cylindrical chamber 45 cm in diameter and 15 cm in height on the axis of the chamber (Fig. 1). The initial hydrogen pressure was 13 and 32.5 Pa. An external winding carrying a current created a magnetic field in the chamber. The component of the field along the chamber axis was H_z. The chamber walls did not conduct electricity. Passage of the current I induced the magnetic-field component $H\varphi$ in the discharge, this component acting as a magnetic piston for ionized gas particles. The experiment involved determination of the velocity of the resulting shock wave from the propagation of the luminous zone. The component H_z of the magnetic field behind the SW and $E\varphi$ in the laboratory coordinate system were measured at two transducer positions ($r = 10$ and 14 cm from the axis of the unit). The experiments revealed a change in the magnetic field immediately in front of the shock wave, this change being connected with the presence of the electrically conducting layer ahead of the wave. Calculations were performed in dimensionless variables. The degree of dissociation was assumed to be zero in front of the shock and unity behind it.

We calculated the parameters of the shock wave by the method of separate trial runs [8]. Here we introduced artificial quadratic viscosity into the formula for pressure (1.11) and we spread the discontinuity over two or three computational cells. One feature of the calculations was the inclusion of electron temperature and ionization kinetics in the same group of Maxwell equations. This was done due to the fact that the electric field in the region ahead of the gas dynamic SW is heavily dependent on both the degree of ionization and electron temperature. For calculations within the group of equations, we used the perturbed parameter method [17].

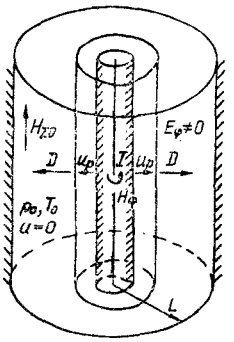

Fig. 1

In [4], the initial value of the magnetic field was 2400 G and the pressure ≳13 Pa. This made it possible to ignore the Hall effect in the calculations, since the latter occurs in the case of stronger fields and lower pressures.

3. Results of Calculations. To analyze the nonsteady propagation of an ionizing SW in a magnetic field, we performed calculations in plane geometry. In this case, the properties of cylindrical geometry are not superimposed on the physical effect of screening of the intrinsic electric field in the particles ahead of the shock. In cylindrical geometry, a nonsteady flow in which u, ρ, and T change develops behind the gas dynamic shock wave.

Three different regimes of propagation of an ionizing SW in a magnetic field were realized, depending on the conditions. For relatively weak SWs (D < 3 km/sec, p_0 ~ 13 Pa, $H_0 \lesssim$ 1 kG), the theory constructed earlier [1-3] works well. Here, advance effects are weakly expressed and ionization takes place behind the shock front (nonbreakdown regime). The magnetic field changes little in the structure of the solution.

In the second and third regimes, electrical breakdown regions develop in front of the shock. Different ionization mechanisms are active in these two regimes. The presence of a conducting region ahead of the shock leads to screening of the electric field. This nonsteady process is described qualitatively by the solution [18]

$$E = E_0 [\exp(-y)(R + \exp(-\tau(1+R)))]^{1/2}[1 + R - \exp(-y)\times (1 - \exp(-\tau(1+R)))]^{-1/2}, \quad (3.1)$$

$$R = 8\pi k J N \alpha_0 u^2/E_0^2, \quad y = 8\pi u \alpha_0 r/c^2 A, \quad \tau = tE_0^2/kJANc^2, \quad A = \alpha/\sigma = \text{const}.$$

Here, E_0 is the intrinsic electric field in the particles at the shock (directly in front of the wave); u is the velocity of the incoming flow in the coordinate system connected with the shock; α_0 is the initial degree of ionization, due (for example) to photoionization. It follows from (3.1) that the electric field weakens (screening takes place) with an increase in r, and the steady state is reached as $t \to \infty$.

The inequality $u_p H_0/(cp_0(E/p_0)_{pr}) > 1$ will serve as the criterion for the existence of a regime with breakdown. In this case, the intrinsic electric field E generated by the wave turns out to be greater than the breakdown value for the gas. As a result, avalanche ionization occurs in the field ahead of the discontinuity. In the second regime involving breakdown, due to the presence of the shock front, the advance radiation creates free electrons to initiate the Townsend ionization process. In this case, proper analysis of the phenomenon requires consideration of absorption of continuous-spectrum radiation in the nonequilibrium region of ionization relaxation behind the shock front and allowance for the non-Maxwellian character of the free-electron-energy distribution function as ionization develops in the electric field in the zone ahead of the shock. Figure 2 shows the distribution of E, H, and α in Lagrangian coordinates at two successive moments of time (denoted by the numbers 1 and 2). Here, S is the region in which the gas dynamic SW was distributed in the calculations, p_0 = 13 Pa, T_0 = 300 K, H_0 = 1200 G, and $u_p = 5 \cdot 10^6$ cm/sec. Figure 3 shows the distribution of T, T_e, and ρ at the moment of time denoted by the number 1 in Fig. 2.

It follows from the calculations (Figs. 2 and 3) that the region of MHD interaction in front of the gas dynamic SW contracts over time (this corresponds to the region of change in E and H in front of S in regimes 1 and 2). The ionization process develops over time, so that grad |E| decreases ahead of the shock. This in turn slows the ionization in front of

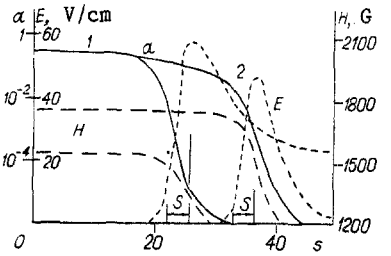

Fig. 2

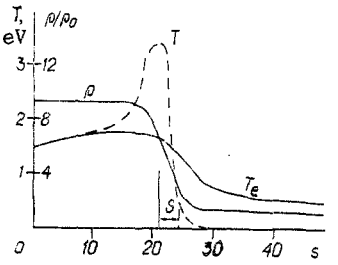

Fig. 3

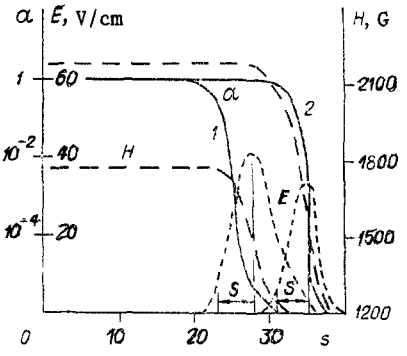

Fig. 4

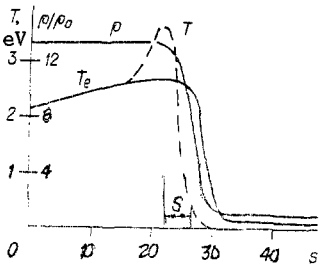

Fig. 5

TABLE 1

Initial and boundary conditions			Experiment			Calculation		
H_0, G	p_0, Pa	u_p, cm/μsec	H_2/H_0	E_l, V/cm	D, cm/μsec	H_2/H_0	E_l, V/cm	D, cm/μsec
2140	32,5	4,2	1	71	4,2	1,05	94,4	4,44
1280	32,5	4,35	1	53	4,65	1,1	61,2	4,98
420	13	4,7	1	18	4,8	1,14	22,5	5,07
420	32,5	5	1	16	5,25	1,21	25,4	5,31
420	13	6,75	1,54	15	7,3	1,61	45,6	7,22
420	13	6,75	2,45	—	7,3	2,78	78,8	7,22
1280	13	6,75	1,3	85	6,7	1,4	120,9	7,12
1280	13	6,75	1,65	79	6,7	1,72	148,6	7,12
2140	32,5	6,25	2,12	138	7,0	2,18	291,6	6,94
2140	32,5	6,25	2,29	139	7,0	2,62	350,4	6,94

the shock and causes the breakdown region to contract. The thickness of the breakdown zone in the calculations was on the order of 4 cm (Fig. 2, with one interval s in the undisturbed region corresponding to about 0.5 cm). The main change in the magnetic field occurs in the breakdown zone. In the third regime, the main source of free electrons is photoionization by advance radiation. Here, the presence of the electric field determines the equilibrium degree of ionization reached in front of the shock during photoionization. Such a situation develops for very strong SWs ($D > 7$ km/sec, $p_0 \sim 13$ Pa), the equilibrium temperature behind such shocks exceeding 2 eV (Figs. 4 and 5). Figure 4 shows the distribution of E, H, and α in Lagrangian coordinates at two successive moments of time, $p_0 = 13$ Pa, $T_0 = 300$ K, $H_0 = 1200$ G, and $u_p = 8 \cdot 10^6$ cm/sec. Figure 5 shows the distribution of T, T_e, and ρ at the moment of time denoted by the number 1 in Fig. 4. Here, it turns out in the calculations that the characteristic photoionization time $\tau \sim 10^{-7}$ sec. Thus, the quantity α in front of the shock can be considered an equilibrium function of T_e. It follows from the calculations that the thickness of the breakdown zone is reduced somewhat, while the screening of E is more pronounced than in the case depicted in Figs. 2 and 3. The time over which the steady state is attained is determined by Eq. (1.6) and turns out to be on the order of the time of the experiment [4]; no steady-state solution is seen. The difference from the second regime involving breakdown is governed by the criterion

$$\frac{\dot{\alpha}_{\text{pht}}}{\dot{\alpha}_{\text{co}}} = \frac{2\pi S_{\text{pht}}(T_2)\exp(-r/l)}{N_0 kJ l \alpha T_a} \approx \frac{10^4 \exp(-J/T_2)}{p_0 A \exp(-Bcp_0/u_p H_0)} \gg 1 \qquad (3.2)$$

$$\left(l \equiv k_\nu^{-1} \quad (1.12), \quad \alpha \sim 1, \; r \approx 0\right),$$

where T_a is calculated for $E/p = u_p H_0/cp_0$; A and B are empirical constants [14] determined for different gases; the radiant flux is determined by the Planck spectrum with $\alpha = \alpha_{eq}$; T_e is the equilibrium temperature behind the gas dynamic SW. In Eq. (3.2), absorption of radiation in the relaxation zone behind the shock is ignored. The mean free path is calculated for the frequencies $\hbar\nu = kJ$. The rate of ionization throughout the breakdown zone is in accordance with the Townsend process.

The most distinctive feature of the solution in cylindrical geometry compared to the plane case is the sharper drop of E to 0 ahead of the shock, by virtue of the geometry of the problem.

Table 1 shows experimental and theoretical values of the parameters in the solution for cylindrical geometry. The theoretical values of H_2 were taken for a moving piston, $E_\ell = u_p H_2$. The fact that they are consistently higher than the experimental values is due in particular to the spreading of the gas dynamic shock wave in the calculations. The velocity of the shock accounts for 10% of the experimental error. The fact that the theoretical values of the electric field in the laboratory coordinate system are greater than the experimental values can be linked to three factors: first, exaggeration of the theoretical value of the magnetic field behind the shock; second, the presumption of a constant piston velocity in the calculations, while the velocity of the magnetic piston in the experiment decreased over time – evidence also of the disagreement of the experimental values of u_p, H_2, and E_ℓ; third, in the experiment, E_ℓ was determined directly behind the shock, where $u < u_p$ by virtue of the geometry of the problem. This leads to underestimation of E_ℓ.

LITERATURE CITED

1. A. G. Kulinkovskii and G. A. Lyubimov, "Magnetohydrodynamics of shock waves ionizing a gas," Dokl. Akad. Nauk SSSR, 129, No. 1 (1959).
2. A. A. Barmin and A. G. Kulikovskii, "Shock waves ionizing a gas in the presence of a randomly oriented magnetic field," in: Problems of Fluid and Continuum Mechanics [in Russian], Nauka, Moscow (1969).
3. A. A. Barmin and A. G. Kulikovskii, "Shock waves ionizing a gas in an electric field," Dokl. Akad. Nauk SSSR, 178, No. 1 (1968).
4. C. F. Sterbins and G. G. Vlases, "An experimental study of transverse ionizing MHD shock waves," J. Plasma Phys., 2, Pt. 4 (1968).
5. F. Y. Sorrell, "Current sheet dynamics in an inverse pinch shock tube," Phys. Fluids, 11, No. 5 (1968).
6. M. I. Hoffert, "Precursor ionization effects on magnetohydrodynamic switch-on structure," J. Plasma Phys., 4, No. 3 (1970).
7. M. A. Liberman and A. L. Velikovich, "Physics of ionizing shock waves in magnetic fields, Phys. Rep., 84, No. 1 (1982).
8. A. A. Samarskii and Yu. P. Popov, Difference Methods of Solving Gas Dynamic Problems [in Russian], Nauka, Moscow (1980).
9. M. A. Tsikulin and E. G. Popov, Radiative Properties of Shock Waves [in Russian], Nauka, Moscow (1977).
10. L. M. Biberman, V. S. Vorob'ev, and I. T. Yakubov, Kinetics of a Nonequilibrium Low-Temperature Plasma [in Russian], Nauka, Moscow (1982).
11. C. D. Mathers, "Transverse MHD shock waves in a partly ionized plasma. Pt. 2. Shock structure in hydrogen," J. Plasma Phys., 23, No. 1 (1980).
12. Yu. P. Raizer, Modern Physics of Gas-Discharge Processes [in Russian], Nauka, Moscow (1980).
13. R. I. Soloukhin, Yu. A. Yakobi, and A. V. Komin, Optical Characteristics of a Hydrogen Plasma [in Russian], Nauka, Novosibirsk (1973).
14. S. Brown, Elementary Processes in a Gas-Discharge Plasma [Russian translation], Atomizdat, Moscow (1961).
15. L. Crompton and R. Huxley, Diffusion and Drift of Electrons [Russian translation], Mir, Moscow (1967).
16. N. N. Pilyugin and G. A. Tirskii, Principles of the Dynamics of a Radiating Gas [in Russian], Izd. MGU, Moscow (1979).

17. T. Shoop, Solution of Engineering Problems on a Computer [Russian translation], Mir, Moscow (1982).
18. V. S. Uspenskii, "Propagation of an ionization wave in front of a shock wave in a magnetic field," in: Mechanics of Deformable Media [in Russian], Izd. MGU, Moscow (1985).

KINETICS OF THERMAL EMISSION FROM AN AEROSOL PARTICLE

N. N. Belov

UDC 537.36:541.182.2/3

One method of supplying seeding electrons during the development of an optical discharge plasma is thermal electron emission from a target surface [1]. The case of a massive target was studied in [1]. The present paper investigates the special features of thermal electron emission from aerosol particles which can be considered as isolated targets. For these there is typically an increase of the retarding electric field as the emitted charge increases [2].

1. Statement of the Problem. With thermal electron emission a steady state is reached in an aerosol as a result of exchange by electrons between particles [2]. The characteristic time to reach thermal emission equilibrium in the aerosol is $>10^{-6}$ sec [2]. Thus, for $t \leq 10^{-6}$ sec, the problem of thermal electron emission in an aerosol reduces to thermal electron emission from an individual particle. In air under normal conditions for a finely dispersed fraction of aerosol the electron mean free path in the gas surrounding the particle considerably exceeds the particle size. And although this relationship breaks down with increase of the particle radius, the process of thermal electron emission from an individual particle under vacuum can be considered as a first approximation for many actual situations. Suppose that the surface temperature of a spherical particle varies according to the formula

$$T = T_0 + (T_k - T_0)\{1 - \exp(-kt/\tau)\}, \tag{1.1}$$

which is appropriate for describing the influence of the processes of heat outflow from a particle with internal heat sources. If we neglect the influence of heat outflow from the particle, then the variation with time of the particle surface temperature can be approximated by a model dependence of the type

$$T = T_0 + (T_k - T_0)(t/\tau)^s. \tag{1.2}$$

Equations (1.1) and (1.2) model the kinetics of the particle temperature for the most important types of particle heating, for example, due to absorption of electromagnetic radiation. Relation (1.2) with s = 1 corresponds to heating of a particle in the case when the particle heat capacity C and the power supplied to the particle W do not depend on the time. With s = 2, Eq. (1.2) describes a linear increase of W with time, with C = const. We can point to real-life analogies for other values of the constants of Eqs. (1.1) and (1.2). As an upper limit of the temperature T_k of the heated particle it is appropriate to take the boiling temperature T_v of the particle material. This is because most of the processes of nonlinear optics postulate high-temperature heating of the particles to T_v. On the other hand, bipolar ionization of the products of evaporation reduce the role of thermal electron emission in the charging of a particle at temperatures greater than T_v.

2. Methods of Numerical Investigation of Particle Charge. The kinetics of the variation of the charge z of the particle is described by the system of equations

$$J \equiv dz/dt = 4\pi a^2 e^{-1} j; \tag{2.1}$$

$$T = T(t), \tag{2.2}$$

where J is the flux of thermal emission electrons from the particle surface; j is the current density from unit particle surface area, determined by the Richardson–Dushman formula

Moscow. Translated from Zhurnal Prikladnoi Mekhaniki i Tekhnicheskoi Fiziki, No. 6, pp. 27-31, May-June, 1989. Original article submitted November 12, 1987; revision submitted February 2, 1988.

 0021-8944/89/3003-0362$12.50